Acta Pharmaceutica Sinica B 2022;12(11):4193–4203

Chinese Pharmaceutical Association
Institute of Materia Medica, Chinese Academy of Medical Sciences

Acta Pharmaceutica Sinica B

www.elsevier.com/locate/apsb
www.sciencedirect.com

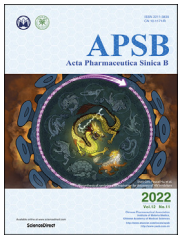

ORIGINAL ARTICLE

Biosynthesis of rumbrins and inspiration for discovery of HIV inhibitors

Beifen Zhong[a,†], Jun Wan[a,†], Changhui Shang[a,†], Jiajia Wen[b], Yujia Wang[b], Jian Bai[a], Shan Cen[b,*], Youcai Hu[a,*]

[a]*State Key Laboratory of Bioactive Substance and Function of Natural Medicines, Institute of Materia Medica, Chinese Academy of Medical Sciences & Peking Union Medical College, Beijing 100050, China*
[b]*Institute of Medicinal Biotechnology, Chinese Academy of Medical Sciences & Peking Union Medical College, Beijing 100050, China*

Received 1 January 2022; received in revised form 24 January 2022; accepted 4 February 2022

KEY WORDS

Rumbrins;
Polyketide;
Precursor-directed biosynthesis;
Resistance gene;
Anti-HIV activity

Abstract Investigation on how nature produces natural compounds with chemical and biological diversity at the genetic level offers inspiration for the discovery of new natural products and even their biological targets. The polyketide rumbrin (**1**) is a lipid peroxide production and calcium accumulation inhibitor, which contains a chlorinated pyrrole moiety that is a rare chemical feature in fungal natural products. Here, we identify the biosynthetic gene cluster (BGC) *rum* of **1** and its isomer 12*E*-rumbrin (**2**) from *Auxarthron umbrinum* DSM3193, and elucidate their biosynthetic pathway based on heterologous expression, chemical complementation, and isotopic labeling. We show that rumbrins are assembled by a highly reducing polyketide synthase (HRPKS) that uniquely incorporates a proline-derived pyrrolyl-CoA starer unit, and followed by methylation and chlorination. Sequent precursor-directed biosynthesis was able to yield a group of rumbrin analogues. Remarkably, inspired by the presence of a human immunodeficiency virus (HIV)-Nef-associated gene in the *rum* cluster, we predicted and pharmacologically demonstrated rumbrins as potent inhibitors of HIV at the nanomolar level. This work enriches the recognition of unconventional starter units of fungal PKSs and provides a new strategy for genome mining-guided drug discovery.

*Corresponding authors. Tel.: +86 10 50927869; fax: +86 10 63017757.
E-mail addresses: shancen@imb.pumc.edu.cn (Shan Cen), huyoucai@imm.ac.cn (Youcai Hu).
[†]These authors made equal contributions to this work.
Peer review under responsibility of Chinese Pharmaceutical Association and Institute of Materia Medica, Chinese Academy of Medical Sciences.

https://doi.org/10.1016/j.apsb.2022.02.005

1. Introduction

Natural products hold vast chemical and biological diversity that cannot be matched by libraries of synthetic compounds, and contribute continually in the fields of biology, chemistry, and medicine[1]. Through biosynthetic evolutionary optimization, natural products tend to be the perfect sources of drug discovery[2]. Understanding the biosynthetic mechanisms of natural products is a key to guiding rational manipulation of nature's biosynthetic machinery to produce natural compounds and their engineered variants[1]. Besides, a deep comprehension of the biosynthetic logic and enzymatic mechanism has created a new field for genome mining-guided discovery of new and bioactive natural products[3−8]. For example, bioinformatic analysis or functional verification of a putative self-resistance gene in a BGC was able to connect the encoded natural products to a potential target[9].

As an important class of natural products in pharmacological science, polyketides have yielded a large number of new drugs for clinical application[4,10], such as lovastatin, rapamycin, and daunomycin. Such success is partly due to the significant variety of polyketide backbones and extensive mechanisms were reported for polyketide scaffolds diversification. For example, a set of catalytic domains including β-ketoreductases, enoyl reductases, and dehydratases can selectively modify the polyketide backbone and a variety of tailoring enzymes are able to modify the polyketide scaffold after it has been assembled by a PKS. While another important diversification step, the incorporation of unconventional starter units, often occurs earlier. Although most of the polyketides are primed with acetyl-CoA, a few PKSs utilize multifarious starter units, such as propionyl acyl carrier protein (CP)[11], 4-coumaroyl-CoA[12], hexanoyl-CoA[13], 2-methylbutyryl-CoA[14], benzoyl-CoA[15], 4-guanidinobutyramide[16], pyrrolyl-CP[17] and 4,5-dichloropyrrolyl-CP[18] (Supporting Information Fig. S1), which in many cases lead to the diverse structural and biological features to the natural products.

Rumbrin (**1**), an unusual chlor-containing polyenylpyrrole, was produced by several fungi from the terrestrial fungal family Onygenales[19] (Fig. 1). Structurally, **1** and its analogs, such as 12*E*-rumbrin (**2**) and auxarconjugatin B (**3**), are featured in an α-pyrone and a pyrrole ring connected by a polyene linker with all *E* or part of *Z* geometrical configuration (Fig. 1). The structural diversity of rumbrins was also constructed by the presence or absence of chlorination on pyrrole moiety and the methyl substitution at different positions on the polyene chain as well as α-pyrone (Fig. 1). Members of this rare class of natural products are usually associated with potent biological activities. For example, **1**, while relatively unstable, was reported to exhibit remarkable cytoprotective and anti-lipid peroxidation activities[19,20]. **2** displays selective cytotoxicity against ovarian cancer cell lines at micromolar level[20], and **3** also show significant cytotoxicity against nonstructural protein (NS-1) cell line[21].

Because of the potent biological activity of **1**, its biosynthesis has attracted broad interesting since its isolation. Although the biosynthetic origin of **1** was proposed and its biosynthetic precursors were subsequently suggested by labeling experiments (Supporting Information Fig. S2)[22,23]. The biosynthesis of **1** and **2** had never been revealed genetically. Herein, we identified the BGC *rum* and characterized the biosynthetic pathway of **1** and **2** through heterologous expression, chemical complementation, and isotopic labeling. Precursors-direct biosynthesis led to the production of a group of rumbrin analogs. Moreover, a putative resistance-like gene *rumB* showing homologous to the gene encoding an HIV-Nef-associated acyl-CoA thioesterase (hACTE-III) in the *rum* cluster was discovered, which led to our inspiration to evaluate rumbrins as anti-HIV agents.

2. Results and discussion

2.1. Bioinformatic analysis of the genome of Auxarthron umbrinum

Recently, we isolated **2** and **3** from the wild type *A. umbrinum* DSM3193, which is the native producer of **1**[19,25]. The structures of **2** and **3** were fully characterized *via* ^{13}C and ^{1}H NMR (see detail in Supporting Information Tables S4 and S6). Regrettably, **1** was not isolated but detectable in our case since it was photosensitive and readily converted to its isomer **2** (Supporting Information Fig. S3).

The entire carbon backbone of **1** and **2** is hypothesized to be assembled from a single HRPKS according to the isotope-labeling studies[22] as well as pathways of structurally related natural products such as citreoviridin[26]. The pyrrole moiety in the structure of **1** and **2** was believed to be derived from proline (**4**) or pyrrole-2-carboxylic acid (**5**)[23]. Considering the high incorporation of **5** into **1** in previous labeling experiments[22], it could be a direct precursor of **1** and **2**. In addition, methylation and halogenation are also required for their biosynthesis (Fig. 2).

For most HRPKSs, there is frequent lack of a domain for product release, instead a acyltransferase-like enzyme or discrete thioesterase (TE) is required to release the product[27]. For instance, a *trans*-acting TE, BerkB, was reported to catalyze the macrolactonization during the biosynthesis of fungal macrolide, A26771B[28]. We deduced that a *trans*-acting TE would exist in the gene cluster of **1** and **2** (Fig. 2). Furthermore, the enzymes responsible for amino acid activation and incorporation are required for constructing the aminoacylated polyketides, such as CoA-ligase and NRPS-like enzyme (Fig. 2)[29], according to the known fungal HRPKS programming rules. Overall, a BGC encoding a HRPKS, a *trans*-acting TE, a CoA-ligase or NRPS-like enzyme, a methyltransferase, a halogenase and additional redox enzymes are necessary during the biosynthesis of **1** and **2**.

To investigate the biosynthetic pathway of **1** and **2**, we sequenced the producer fungus *A. umbrinum* DSM3193. Bioinformatic analysis revealed that the BGC located in scaffold 127 is the only candidate qualifying the **1** and **2** biosynthesis and is named *rum* cluster (Fig. 3A and Table S3). With the aid of RT-PCR, we defined the *rum* cluster to contain 10 genes (Fig. S3), which encode a transcriptional regulatory (TF, RumA), an hACTE-III (RumB), a CoA-ligase (RumC), a HRPKS (RumD) with six domains (KS-AT-KR-DH-MT-ACP), a discrete TE (RumE), a methyltransferase (RumF), a 2-oxoglutarate-dependent dioxygenase (α-KGD, RumG), a flavin-dependent halogenase (RumH) and three uncharacterized proteins, respectively.

2.2. Characterization of rum cluster for rumbrin biosynthesis

According to the known mechanism for pyrrole biosynthesis, pyrrolyl-CoA or pyrrolyl-CP is usually derived from proline through oxidation. The pyrrole moiety in rumbrin was also suggested to be derived from proline based on ^{15}N-labeled precursor[22]. To further confirm the biosynthetic origin of pyrrole ring in **1** and **2**, we used the full labeled $_{L}$-proline-[$^{13}C_5$,^{15}N] to perform

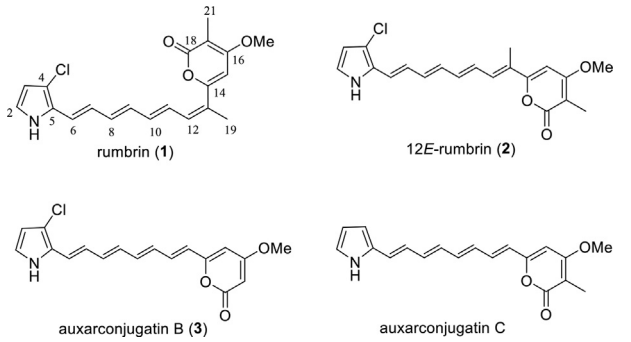

Figure 1 Chemical structures of rumbrin (**1**) and its analogues.

the feeding experiment. As a result, an increase of 6 mu in molecular weight of **2** and **3** were detected by mass spectrometry (Supporting Information Fig. S5). This revealed that five ^{13}C and one ^{15}N from L-proline-[$^{13}C_5$,^{15}N] were all incorporated into **2** and **3**, which further confirmed that the pyrrole moiety in **2** was initially originated from proline (**4**).

Subsequently, to confirm the *rum* gene cluster and elucidate the biosynthetic pathway of **1** and **2**, gene knockout experiments in *A. umbrinum* were carried out firstly. Nevertheless, all attempts to knockout genes in the *rum* cluster failed. We then turned to heterologously express the *rum* genes in the host *Aspergillus nidulans* A1145. Expression of *rumD*, *rumDE*, *rumCD* and even *rumCDE* separately in *A. nidulans*, supplying proline (**4**, 2 mmol/L), did not yield any new products compared to the *AN-control* (data not shown). While the transformant *AN-rumCDE* feeding with **5** produced additional peaks **6**−**8** detected by LC−MS analysis (Fig. 3B, trace ii), which were later identified as 16-demethyl-auxarconjugatin D, 13-methyl-16-demethyl-auxarconjugatin D, and 16-demethyl-dechloroisorumbrin respectively, *via* 1D and 2D NMR (Supporting Information Tables S4 and S6). These results not only confirm the *rum* cluster was responsible for the biosynthesis of **1** and **2**, but also supported our proposal that oxidation of proline occurred before the polyketide chain elongation (Fig. 2). The results that the strains *AN-rumD*, *AN-rumDE* and *AN-rumCD*, which did not produce any new products, while the strain *AN-rumCDE* did (Supporting Information Fig. S6, traces ii-v), also suggests that RumC activates substrate, HRPKS RumD assembles a C17 polyketide chain through six iterations of malonyl-CoA extension, and RumE catalyzes the lactonization of the C17 polyketide chain (Fig. 3C).

2.3. *Oxidation catalyzed by a 2-oxoglutarate-dependent dioxygenase, RumG*

It was reported that a dehydrogenase was sufficient to convert proline to pyrrole ring in bacteria[30,31]. While the homologous protein of RedW, which is a dehydrogenase that catalyzes the conversion from prolyl-CP to pyrrolyl-CP in bacteria (Supporting Information Fig. S7)[32], was not found among the proteins encoded by the *rum* cluster. Instead, an α-KGD (RumG) with sequence homology to EcdG (28%), which was suggested to catalyze the hydroxylation of proline in the biosynthesis of echinocandin B, was shown in *rum* cluster. As the only redox enzyme in *rum* cluster, RumG was postulated to be involved in the oxidization of proline to form pyrrole ring. To investigate its role, the gene *rumG* was introduced into the strain *AN-rumCDE* feeding with **4**. After 4 days of culture, a major product **8** together with minor products **6** and **7** were detected by LC−MS (Fig. 3B, trace iii). This supported our hypothesis that RumG catalyzed the formation of tetrahydropyrrole ring to pyrrole ring (Fig. 3C). To test whether **4** was the direct substrate of RumG, we heterologously expressed *rumG* in *A. nidulans* and cultured it in a proline-containing CD-ST media. Unfortunately, the desired product **5** was not detected (Supporting Information Fig. S8), which lead to our postulation that CoA thioester instead of free proline may be the natural substrate for RumG (Fig. 3C).

2.4. *Post-PKS modification*

Next, we focused on the function of the methyltransferase RumF and the halogenase RumH. Co-expression of *rumCDEGF* feeding with **4** led to the production of three new metabolites **9**−**11** (Fig. 3B, trace iv), which were purified and characterized as auxarconjugatin D (**9**), 4-dechloro-17-demethyl-isorumbrin (**10**), and 12*E*-dechloroisorumbrin (**11**), respectively. The identification of **9**−**11** with 16-*O*-methylated structures highly suggested that RumH was responsible for the *O*-methylation at C-16. While the strain *AN-rumCDEGH* produced minor products **12**−**13** and major product **14** (Fig. 3B, trace v), in which **13** and **14** were fully identified as 12*E*-demethylisorumbrin and 16-demethyl-isorumbrin by NMR, respectively. Although **12** was

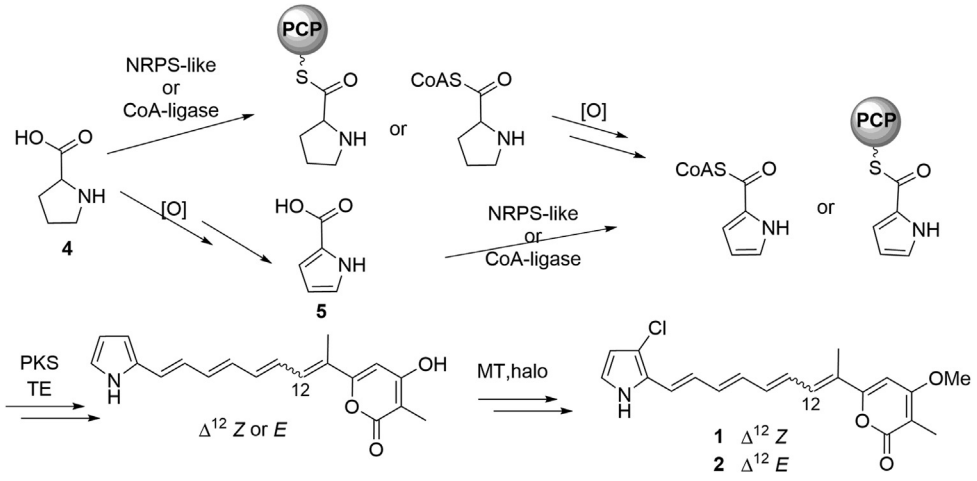

Figure 2 Proposed biosynthetic pathway of **1** and **2**.

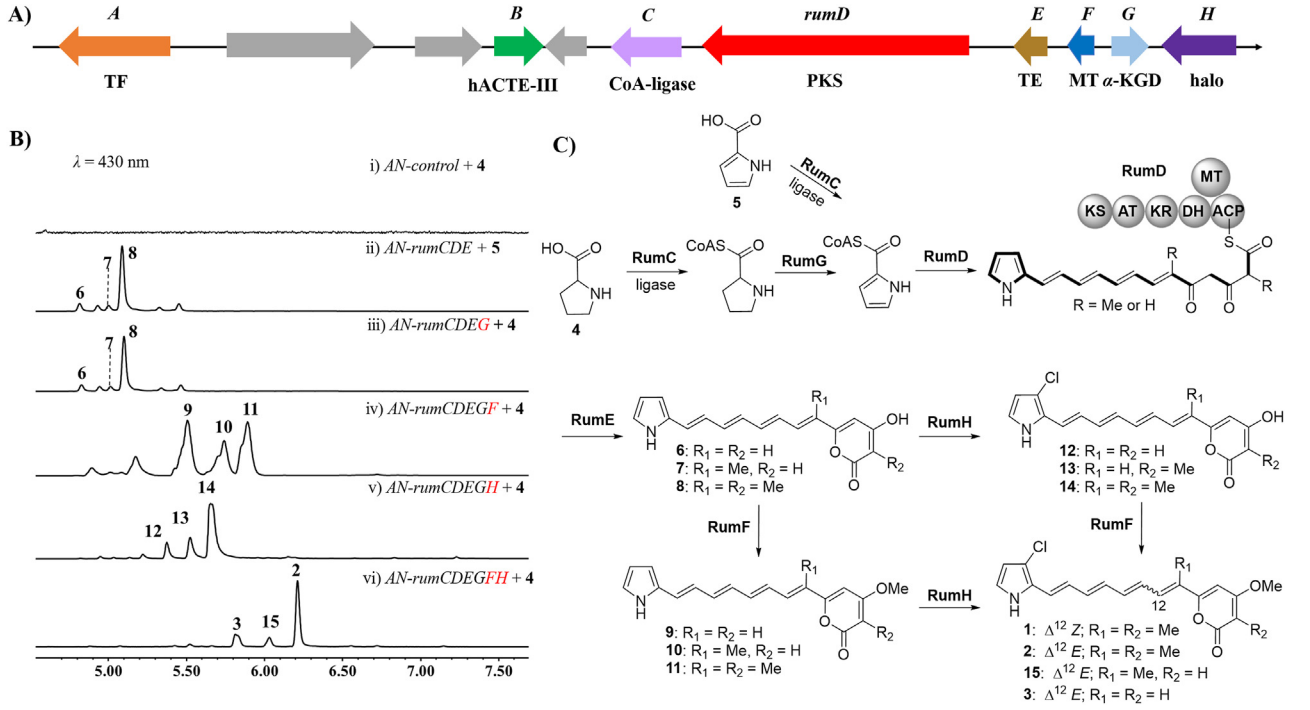

Figure 3 Identification of the BGC and pathway of **1** and **2**. (A) The *rum* gene cluster in *A. umbrinum*. (B) LC−MS analysis of products profiles of heterologous expression of different combinations of *rum* genes in *A. nidulans*. (C) Putative biosynthetic pathway of **1** and **2**. AT, acyl transferase; ACP, acyl-carrier protein; DH, dehydratase; KS, ketoacyl synthase; KR, ketoreductase; MT, methyltransferase.

not purified, its molecular weight and UV indicated this is the chlorinated **6**. This suggested RumH was responsible for the chlorination at C-4.

To determine whether chlorination happened after the formation of polyketide skeleton, **4** and **5** were separately fed as substrate to the culture of strain *AN-rumH*. As a result, no chlorinated products could be detected in both cases (Supporting Information Fig. S9). Actually, RumH was phylogenetically close to a halogenase, MalA, which also catalyzed the chlorination of an off-line substrate in the biosynthetic pathway of malbrancheamide[33] (Supporting Information Figs. S10 and S11). Combined with the low incorporation of 3-chloropyrrole-2-carboxylate into **1** in the previous report[22], it is reasonable that the chlorination was a post-PKS modification step.

To further determine the function order of RumH and RumF, we performed feeding experiments. Upon supplementing the mixture of **6**−**8** or **9**−**11** to *A. nidulans* expressing RumH, the corresponding chlorinated products were detected (Supporting Information Fig. S12, traces i and ii). Furthermore, the mixture of **6**−**8** or **12**−**14** was converted to the corresponding *O*-methylated products in the presence of RumF (Fig. S12, traces iii and iv). These results suggested that the methylation and halogenation could occur simultaneously during the biosynthesis of **1** and **2**. As a trial, both RumF and RumH were added to the strain *AN-rumCDEG* feeding with **4**, and the production of major **2** along with minor **3** and **15** were observed (Fig. 3B, trace vi), which also supported our proposal.

Hence, the overall biosynthetic pathway of **1** and **2** in *A. umbrinum* could be deduced (Fig. 3C). Beginning with the conversion of proline to prolyl-CoA by a CoA-ligase, an α-KGD oxidizes prolyl-CoA to form pyrrolyl-CoA, and the PKS and discrete TE could utilize pyrrolyl-CoA and malonyl-CoA as building blocks to construct polyketide backbone, which can be *O*-methylated and chlorinated to give **1** and **2**.

2.5. *Precursor-directed biosynthesis*

As a feasible strategy, precursor-directed biosynthesis is frequently used to construct new functional groups to improve structural diversity, which usually impacts the bioactivity of the compound[34] or provide a functionalizable handle for structural modification[35]. Encouraged by fact that CoA-ligase RumC was able to recognize different substrates as mentioned earlier[23], a panel of commercially available analogues of **5** (Supporting Information Fig. S13) were separately fed into the culture of the strain *AN-rumCDE* and *AN-rumCDEFH*, to produce rumbrin derivatives. As a result, among all the substrates fed, 4-bromo-, 4-fluoro-, and 3-fluoro-pyrrole-2-carboxylic acids can be converted into new products, while switching the pyrrole ring to thiophen, furan, or pyridine ring did not yield any new products, as detected by LC−MS (Supporting Information Fig. S14). Finally, a total of nine products (**16**−**24**, Fig. 4) were isolated and structurally characterized by MS and NMR.

2.6. *Resistance-like gene-directed anti-HIV evaluation*

Self-resistance genes are continually reported from microbial natural product BGC[7,36,37]. This phenomenon has been frequently used to identify BGCs of natural products with known bioactivities, as well as to predict bioactivity and molecular target of

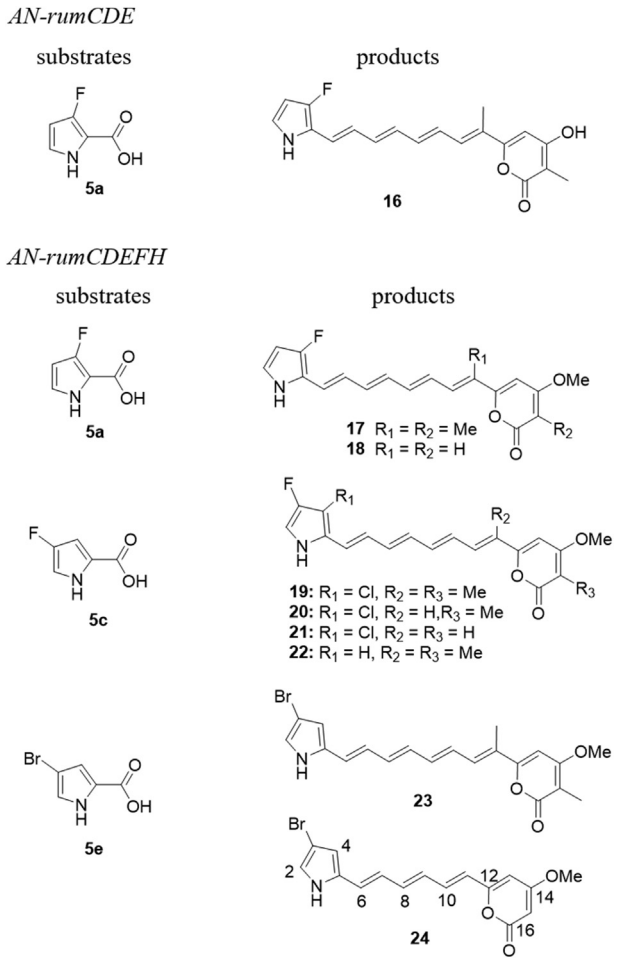

Figure 4 Precursor-directed biosynthesis of rumbrin analogs.

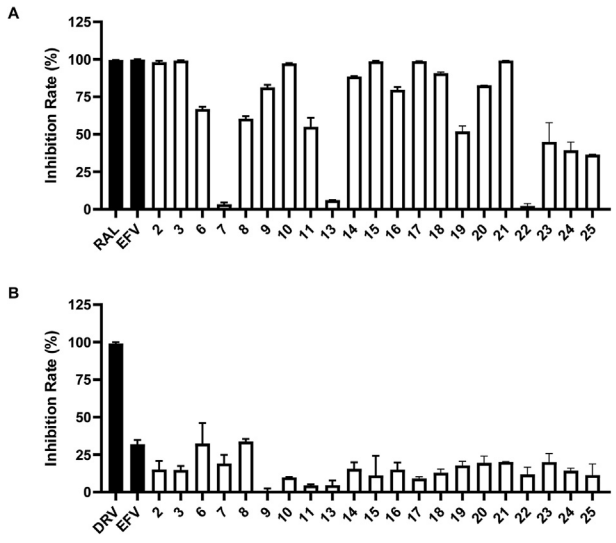

Figure 5 Rumbrins potentially inhibit the early stage of HIV-1 replication. (A) HIV-1 NL4-3luc.R-E- pseudoviruses were used to infect SupT1 cells in the presence of test compounds. The infected cells were lysed followed by the measurement of luciferase activity. EFV and RAL were used as controls; (B) HEK293T cells were transfected with pNL4-3luc.R-E- in the presence of test compounds or DMSO. The resulting virus particles were collected and infected SupT1 cells, followed by measuring luciferase activity to determine viral infectivity. As controls, protease inhibitors (PIs) darunavir (DRV), as well as inactive control EFV were also tested; Data represent the mean ± SD of three independent experiments.

natural products[8,38–42]. Remarkably, phylogenetic analyses revealed that RumB, differs from classical TE, belongs to TesB-like subfamily (Supporting Information Figs. S15 and S16) and shows homolog to *Escherichia coli* thioesterase II (32%), and human thioesterase II (hTE, 33%)[43]. It seems that RumB does not involve in the biosynthetic steps toward **1** and **2** based on bioinformatic analysis. Indeed, when *rumB* was introduced into the strain *AN-rumCDEFGH*, neither any additional products were produced nor yield of rumbrins increased (data not shown). The results from bioinformatic analysis and heterologous expression inspired our suspicion that *rumB* may function as a resistance-like gene.

Of note, hTE has been reported to be an important cellular partner of HIV-1 Nef and suggested to play several roles in HIV-1 infectivity[44,45]. Therefore, the possible interplay between hTE and the compounds from *rum* cluster suggests their potential anti-HIV-1 bioactivity. Subsequently, all the rumbrin analogs obtained from this study were evaluated for their inhibition activity against HIV-1. As a result, most of the test compounds significantly inhibited the HIV-1 infection in the early stage of a one-cycle HIV-1 infection assay (Fig. 5A). In detail, compounds **2**−**3**, **9**−**10**, **14**−**15**, **17**−**18**, and **20**−**21** possess over 80% inhibition rate at 10 μmol/L concentration and IC_{50} among 20.9−376.6 nmol/L (Supporting Information Table S11). It seems that the presence of 16-*O*-methyl and/or 4-Cl group contribute significantly to their anti-HIV activity. To assess the effect of the compounds upon the late stage of HIV-1 replication, which includes the steps from gene expression to virus production, HEK293T cells were transfected with pNL4-3luc.R-E- and VSVg in the presence of test compounds or DMSO. Then, supernatant virus particles were collected and infected SupT1 cells. Meanwhile, rumbrins (Fig. 5B) had little effect on HIV-1 infection in the late stage. Taken together, these data suggest that rumbrins potently interrupt the early step of viral replication.

To explore the mechanism how these compounds inhibit the early stage of viral replication, which includes viral entry, reverse transcription and integration, we next assess their effect upon viral reverse transcription and integration using relative quantitative PCR (RQ-PCR). Primers were designed to detect U5-Gag, Alu-LTR and 2-LTR sequences, which were indicative of reverse transcription products, integrated viral DNA and 2-LTR-containing DNA circles, respectively. SupT1 cells were infected with pseudotyped HIV-1 in the treatment of DMSO, EFV, RAL, or the most active compound **2**. As shown in Fig. 6A, **2** did not affect the level of U5-Gag products, suggesting that **2** had no inhibitory effect upon reverse transcription. In contrast, compound **2** markedly reduced the level of integrated viral DNA, supporting an inhibition on viral integration (Fig. 6B).

2-LTR circles form at a low level in the nucleus through the action of cellular nonhomologous DNA end joining, blockage to HIV-1 integration would result in an increasing level of 2-LTR circles after nuclear entry of HIV-1 cDNA[46]. Therefore, the level of 2-LTR circles is considered as an indicative for the nuclear import of pre-integration complex. Indeed, the number of 2-LTR circles was 3.7-fold higher in RAL-treated cells compared with

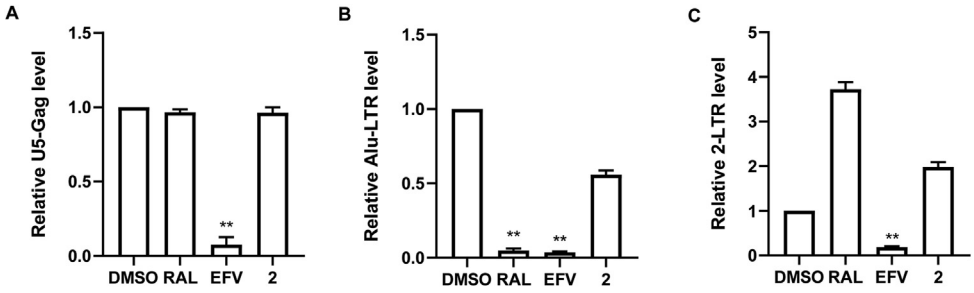

Figure 6 12*E*-Rumbrin (**2**) inhibits HIV-1 replication by blocking viral integration. (A−C) VSV-G pseudotyped NL4-3Luc R-E- viruses were used to infect SupT1 cells with the treatment of DMSO, 4 nmol/L EFV, 25 nmol/L RAL, or **2**. HIV-1 RT DNA (A), integrated DNA (B), and 2-LTR circles (C) were quantified by RQ-PCR using the corresponding primers (Table S1). $*P < 0.05$.

DMSO-treated control cells (Fig. 6C). The number of 2-LTR circles in **2** group was 2 times higher than that of the DMSO group (Fig. 6C). Together, these data suggest that compound **2** inhibit HIV-1 replication by blocking viral integration, while other possible anti-HIV mechanism awaits further investigation.

2.7. *Discussion*

Proline-derived pyrrolyl-CP, an unconventional starter unit of PKS, was reported to be originated from an NRPS-like pathway in bacteria. The selective adenylation of proline by a prolyl-AMP ligase, loading onto the discrete CP, yielding prolyl-*S*-CP, which was then converted into pyrrolyl-CP by prolyl-*S*-CP dehydrogenase, in an FAD-dependent manner (Fig. S7)[17]. Nonetheless, pyrrolyl act as a starter unit has never been verified genetically in fungal PKS systems. In our case, while we did not completely clarify the biosynthesis mechanism of pyrrolyl-CoA, we suggested a new pathway for pyrrolyl-CoA formation which is completely different from the pyrrolyl-CP biosynthesis well-known in bacteria. In detail, a CoA-ligase RumC activates substrate, then the α-KGD RumG catalyze the oxidation of both sides of the prolyl-CoA or, alternatively, hydroxylate C4 and followed by spontaneous dehydration to form Δ^4-pyrrolinyl-2-carboxyl-CoA intermediate, which was oxidized to the pyrrolyl-CoA spontaneously. Comparing to the biosynthesis of pyrrole-CP in bacteria, fungi take a more convenient pathway. Our study shed light on the biosynthesis of pyrrole-containing natural compounds. Admittedly, *in vitro* assay was expected to completely clarify the biosynthesis mechanism of pyrrolyl-CoA and further study on the RumG is ongoing in our lab.

The presence of a self-resistance gene in a BGC opens a new window for the prediction of the bioactivity of natural products synthesized by the biosynthetic pathway. Here, we predicted that rumbrins have anti-HIV activity according to the existence of a potential self-resistance gene *rumB* in the *rum* cluster. Even though it would be more convincing if hTE is proved to be the target of rumbrins, the potent inhibition against HIV-1 by rumbrins provides evidence supporting the efficiency of self-resistance gene-guided bioactive natural product discovery. Interestingly, a gene cluster *mas* homologous to *rum* was found in *Malbranchea sulfurea*. The absence of homolog to *rumB* in *mas* cluster suggested the products from this cluster may not possess anti-HIV activity. Indeed, heterologous expression of the *mas* cluster in *A. nidulans* led to the production of a rumbrin analog, **25**, with a shorter polyene linker (Supporting Information Fig. S17), and it showed very weak anti-HIV activity in the bioassay, which highly suggested the presence of *rumB* is connective to the anti-HIV activity of rumbrin. Interestingly, RumB, a protein from a soil fungus, shows homologous to hTE, which is widely distributed from prokaryotes to eukaryotes[47,48]. Its function in the biosynthesis of rumbrin is unknown and deserves further study.

Notably, early studies reveal that the interaction of Nef and hTE plays an important role in the down-regulation of CD4 and MHC-I[47,49], while the function of hTE in HIV-1 replication is still largely unexplored and inconclusive, because of its diverse biological functions including the recycling and sorting of membrane proteins, the lipid metabolism and the β-oxidation. This work raises a possibility that hTE may involve in HIV-1 integration and act as a potential target for the development of anti-HIV therapeutics.

3. Conclusions

In summary, we successfully characterized the genetic basis for rumbrins biosynthesis, and proposed that a new starter unit containing pyrrole ring was incorporated by fungal PKS. This led to the generation of a series of rumbrin analogs by precursor-directed biosynthesis. Based on the existence of a resistance-like gene *rumB* homologous to the gene encoding an HIV-Nef-associated acyl-CoA thioesterase, we predicted and pharmacologically demonstrated rumbrins as potent anti-HIV agents. Our study opens a new window for gene mining-guided drug discovery.

4. Experimental

4.1. *General materials*

TRIZOL® Reagent (Invitrogen, Carlsbad, CA, USA) and the plant genomic DNA extraction kit (Tiangen, Beijing, China) were used to prepare the RNA and genomic DNA of *A. umbrinum*, respectively. DNA *de novo* sequencing was performed at SHBIO (Shanghai, China) using the IIIumina Hiseq Xten platform. Primer synthesis was performed by Genscript Biotech Corporation (Beijing, China). Zymoprep™ Yeast Plasmid Miniprep I Kit (Zymo Research, Orange County, CA, USA) was used to extract plasmids from yeast. Q5 high-fidelity DNA polymerase (New England Biolabs, NEB) or 2 × Hieff® PCR Master Mix (YEASEN, Shanghai, China) was used to carry out polymerase chain reactions (PCR). An Mx3000P real-time PCR system (Agilent Technologies Inc., Palo Alto, CA, USA) was used to perform real-time PCR. DNA restriction enzymes were purchased from NEB. DNA sequencing was performed by BGI Tech Solutions (Beijing Liuhe) Co., Ltd. (Beijing, China). *E. coli trans*1-Blue and *trans*2-

Blue were produced by Transgen Biotech (Beijing, China). Potato dextrose broth medium (PDB) and potato dextrose agar medium (PDA) were produced by BD Difco (Sparks, NV, USA). Cells were collected by centrifuging (Sigma 3-18K, Gettingen, Germany). DNeasy Blood & Tissue Kit (Qiagen, Hilden, Germany) was used to extract the total DNA of SupT1 cells. The HEK293T and SupT1 cells were purchased from ATCC.

Thermo Nicolet 5700 FT-IR spectrophotometer (Waltham, MA, USA) was used for IR spectra measurement. Bruker Avance III 800, Model Avance DMX 700 or Ascend 600 (Bruker Corp., Karlsruhe, Germany) NMR instruments was used for NMR spectra measurement with TMS as internal standard and DMSO-d_6 as solvent. UV spectra were recorded using the JASCO V-650 instrument (JASCO, Corp., Tokyo, Japan). Agilent 1100 Accurate-Mass Q-TOP LC−MS spectrometer (Agilent Technologies, Ltd., Santa Clara, CA, USA) and an LTQ-FT Ultra ESI-FTICR-MS spectrometer (ThermoFisher Scientific, CA, USA) were used for recording HRESIMS data. LC−MS analyses were carried out on an Agilent Infinity II Prime LC with a DAD detector and a G6125B LC/MSD mass detector, or a Waters ACQUITY H-Class UPLC−MS (Milford, MA, USA) with a PDA detector and a QDA mass detector (ACQUITY UPLC® BEH, C18 column, 1.7 μm, 50 mm × 2.1 mm), using positive and negative mode electrospray ionization with a linear gradient of 5%−99% (*v*/*v*) acetonitrile (MeCN)/H_2O in 8 min followed by 99% MeCN/H_2O (both with 0.02% formic acid, *v*/*v*) for 4 min. The flow rate was 0.4 mL/min. Semi-preparative HPLC was carried out using a Silgreen ODS column (5 μm, 250 mm × 10 mm) in a LabAlliance SSI series III HPLC (Scientific Systems Inc., Philadelphia, PA, USA) with UV detector. Analytical grade solvents were used for extraction, HPLC grade MeCN and CH_3OH were used for semi-preparation HPLC separation, and LC−MS grade MeCN was used for LC−MS analysis.

4.2. Strains and culture conditions

The fungus *A. umbrinum* DSM3193 was cultivated on PDA (BD) at 25 °C and stocked in −80 °C with 20% glycerol. For the production of secondary metabolites and RNA extraction, it was grown in PDB (BD) at 25 °C for 7 and 3 days, respectively. *A. nidulans* A1145 was cultured on CD plate (1.52 g/L KH_2PO_4, 6 g/L $NaNO_3$, 0.52 g/L $MgSO_4 \cdot 7H_2O$, 0.52 g/L KCl, 10 g/L glucose, 20 g/L agar, and 1 mL/L trace elements solution) with supplementation of 10 mmol/L uridine, 0.5 mg/L pyridoxine, 5 mmol/L uracil and 2.5 mg/L riboflavin for the collection of spores and the spores were stored at −80 °C in 20% glycerol. *A. nidulans* was grown on CD-ST medium (6 g/L $NaNO_3$, 20 g/L tryptone, 20 g/L soluble starch, 1.52 g/L KH_2PO_4, 0.52 g/L KCl, 0.52 g/L $MgSO_4 \cdot 7H_2O$, 1 mL/L trace elements, 20 g/L agar) to heterologously express the gene cluster and produce compounds. To construct the *A. nidulans* overexpression plasmids, *Saccharomyces cerevisiae* BJ5464-NpgA was used for yeast DNA recombination cloning. Yeast extract peptone dextrose (YPD) medium (10 g/L yeast extract, 20 g/L peptone, 20 g/L dextrose) and the uracil-dropout semisynthetic medium were used for routine growth and selection of plasmids transformed into *S. cerevisiae*, respectively. *E. coli trans*1-Blue and *trans*2-Blue (Transgen Biotech) were used for routine cloning. *E. coli* strains were cultured at 37 °C in LB media (5 g/L yeast extract, 10 g/L NaCl, 10 g/L tryptone, and 20 g/L agar for solid cultivation). The concentration of ampicillin in the media was 100 μg/mL. Plasmids and primers are described in Supporting Information Tables S1 and S2.

4.3. Sequencing and bioinformatic analysis

The genomic DNA of *A. umbrinum* was prepared using the Plant Genomic DNA Kit (Tiangen). Gene clusters were analyzed by 2ndFind (http://biosyn.nih.go.jp/2ndfind) analysis and anti-SMASH (https://fungismash.secondarymetabolites.org). The open reading frames of gene clusters were predicted and manually checked by comparison with known proteins using NCBI Blast tools. Functional domains of PKS were analyzed in PKS/NRPS Analysis Website (http://nrps.igs.umaryland.edu).

4.4. General molecular biology experiments

Restriction enzyme digestion using DNA restriction enzymes recommended by the manufacturer (NEB). DNA sequencing were used to confirm the PCR products and plasmid DNAs.

4.5. Reverse transcription-PCR (RT-PCR)

Mycelia of *A. umbrinum* were frozen with liquid nitrogen, then broken by grinding and dissolved in 1 mL Trizol (Invitrogen). The mixture was added with 200 μL chloroform, vortexed and centrifuged for 15 min at 12,000 rpm. An equal volume of isopropanol was added to the supernatant, then RNA was precipitated and was washed with 75% ethanol and resuspended in 40 μL RNase-free water. The genomic DNA was digested with RNase-free DNase (Promega). Then the cDNA was obtained by RT-PCR using PrimeScirpt™ RT reagent kit (Takara). The cDNA template was used to detect gene expression level by PCR.

4.6. Heterologous expression of the rum gene cluster in A. nidulans

For heterologous expression in *A. nidulan*, plasmids pANP, pANR, and pANU, which contained auxotrophic markers for pyridoxine (*pyroA*), riboflavin (*riboB*) and uracil (*pyrG*), respectively, were used as vectors to insert genes. *glaA*, *gpdA*, and *amyB* were inserted as promoters. Genes from the *rum* cluster with their terminators (~300 bp) were amplified from genomic DNA extract from *A. umbrinum* with overhang primers (Table S1). pANR and pANP were digested with *Bam*HI and PacI. pANU was double-digested with *Bam*HI and *Not*I. The digested vector, corresponding promoters and overlapping DNA fragments were assembled in *S. cerevisiae* BJ5464-NpgA by yeast homologous recombination. The correct colonies were checked by colony-PCR. The plasmids extracted from yeast were transformed into *E. coli trans*1-Blue or *trans*2-Blue for propagation. The correct *E. coli* were transformants checked by colony-PCR. The plasmids extracted from *E. coli* were checked by enzymatic digestion and sequencing.

To obtain the protoplasts of *A. nidulans*, the spores of *A. nidulans* were inoculated into 30 mL liquid GMM medium (1 mL/L trace elements, 0.52 g/L KCl, 10 g/L glucose, 0.52 g/L $MgSO_4 \cdot 7H_2O$, 10 g/L yeast extract, 6 g/L $NaNO_3$, 1.52 g/L KH_2PO_4), which supplemented with 5 mmol/L uracil, 10 mmol/L uridine, 2.5 mg/L riboflavin, and 0.5 mg/L pyridoxine, and germinated at 37 °C, 220 rpm for 5−7 h. The germlings were harvested by centrifugation at 4000 rpm, 4 °C for 6 min, and washed with 25 mL osmotic buffer (0.6 mol/L $MgSO_4$, 10 mmol/L sodium phosphate buffer, pH 7.0). Then, the germlings were resuspended in 10 mL osmotic buffer which containing 20 mg yatalase (Takara) and 30 mg lysing enzymes (Sigma−

Aldrich) and incubated at 80 rpm for 7−8 h at 30 °C for enzymatic digestion. The mixture was transferred to a 50 mL tube and slowly added of 10 mL trapping buffer (0.1 mol/L Tris-HCl, 0.6 mol/L sorbitol, pH 7.0). And then centrifugation at 3750 rpm, 4 °C for 15 min, the protoplasts at the middle layer were transferred to a new tube and washed with doubled volumes of STC buffer (1.2 mol/L sorbitol, 10 mmol/L Tris-HCl, 10 mmol/L $CaCl_2$, pH 7.5). After centrifugation at 3750 rpm, 4 °C for 5 min, the protoplasts were then resuspended in a suitable volume of STC buffer for transformation. For single transformation, firstly, plasmids were added into 100 μL of protoplasts and incubated on ice for 50 min. Then the mixture was added to 600 μL PEG solution (10 mmol/L Tris-HCl, 60% PEG4000 and 50 mmol/L $CaCl_2$, pH 7.5) and lightly mixed, incubated 20 min at 25 °C. Finally, the mixture was transferred to CD-sorbitol medium (6 g/L $NaNO_3$, 0.52 g/L $MgSO_4{\cdot}7H_2O$, 0.52 g/L KCl, 1.52 g/L KH_2PO_4, 10 g/L glucose, 1 mL/L trace elements solution, 20 g/L agar and 1.2 mol/L sorbitol) and cultured at 37 °C for 2 days.

The picked transformants were inoculated into solid CD medium and cultured at 37 °C for 3−4 days to harvest spores. Three empty plasmids were transferred into the strain *AN-control*, which was used as the control in this study. The spores were inoculated into CD-ST medium for 4 days at 25 °C. Then, the medium was extracted with ethyl acetate (EtOAc). The EtOAc extracts were evaporated to dryness, and then redissolved in methanol (CH_3OH) and subjected to LC−MS analysis.

4.7. Feeding experiments

4.7.1. Feeding experiments in A. nidulans

The transformed *A. nidulans* strains were inoculated in CD-ST medium, with L-proline (**4**, 2 mmol/L) or pyrrole-2-carboxylic acid (**5**, 2 mmol/L), for 4 days at 25 °C. To determine the function order of RumF and RumH, a mixture of **6**−**8**, or **9**−**11**, or **12**−**14** was fed to the corresponding strains for 4 days at 25 °C. After 4 days, the medium was extracted with EtOAc and analyzed by LC−MS.

4.7.2. L-Proline-[$^{13}C_5$,^{15}N] feeding studies

A. umbrinum was cultured in 30 mL YPD media and cultivated at 28 °C, 220 rpm. 2 mmol/L L-proline-[$^{13}C_5$,^{15}N] or proline used as substrates were added in 3rd day. The mycelia were collected after 7 days, followed by extraction with EtOAc and analysis by LC−MS.

4.8. Precursor-directed feeding studies

Precursors (dissolved in DMSO) were introduced to the CD-ST medium of corresponding heterologously overexpressed *A. nidulans* strains with a final concentration of 2 mmol/L. The cultures were exhaustively extracted with EtOAc on the 4th day, and the extracts were analyzed by LC−MS.

4.9. Isolation and structural characterization of metabolites

To isolate 12*E*-isorumbrin (**2**) and auxarconjugatin A (**3**), *A. umbrinum* was cultured in 500 mL of seed medium (uracil dropout) at 180 rpm, for 2 days at 28 °C. Then the seed culture was inoculated into 10 L production medium at 220 rpm, for 10 days at 28 °C. The culture was filtered and the mycelia were extracted with EtOAc. The resulted crude residue (17 g) was subjected to MCI gel column chromatography eluted with a gradient of CH_3OH/H_2O (20:80, 50:50, 70:30 and 100:0) to give five subfractions (Frs. A−E). Fr. D was subjected to flash chromatography on an ODS column (solvent gradient: 0−20 min, 70% CH_3OH/H_2O; 20−110 min, 70%−100% CH_3OH/H_2O; 110−130 min, 100% CH_3OH/H_2O) to afford Frs. D1−D15. Fraction Fr. D9 (446.6 mg) was separated by a Sephadex LH-20 column (CH_3OH) to obtain Frs. D9A−D9E. Fr. D9D (190 mg) was purified by semi-preparative HPLC (CH_3OH/H_2O, 80:20) to obtain **2** (6.0 mg, t_R = 37.5 min) and **3** (1.0 mg, t_R = 20.5 min).

12*E*-Isorumbrin (**2**): red powder; ESI-MS *m/z* 356 $[M-H]^-$. ^{13}C and ^1H NMR data are shown in Tables S4 and S6.

Auxarconjugatin B (**3**): red powder; ESI-MS *m/z* 324 $[M-H]^-$. ^{13}C and ^1H NMR data are shown in Tables S4 and S6.

To isolate compounds **6**−**8**, the spores of strain *AN-rumCDE* were inoculated into 5 L CD-ST agar media containing **5** (2 mmol/L) as substrate and grown for 7 days at 25 °C. The culture was exhaustively extracted with EtOAc to give the crude extract, which was partitioned between CH_3OH and petroleum ether (PE) (1:1, *v/v*). The CH_3OH layer extract was purified by BUCHI REV Prep with a gradient subjected CH_3OH/H_2O (30:70 to 100:0) to afford four fractions (Frs. 1−4). Fr. 3 was separated by semi-preparative HPLC (CH_3OH/H_2O, 68:32) to obtain **6** (1.2 mg, t_R = 19.0 min), **7** (0.8 mg, t_R = 23.5 min), and **8** (7.0 mg, t_R = 32.5 min).

Compound **6**: red powder; UV (MeCN) λ_{max} (log ε) 267 (4.22), 318 (4.13), 334 (4.28), 434 (4.75) nm. IR ν_{max} 3429, 2960, 2919, 2851, 1722, 1621, 1566, 1543, 1468, 1432, 1415, 1261, 1097, 1035, 863, 802, 720 cm^{-1}. ^{13}C and ^1H NMR data are shown in Tables S4 and S6. ESI-MS *m/z* 282 $[M+H]^+$ and 280 $[M-H]^-$. HRESIMS *m/z* 282.1119 $[M+H]^+$ (Calcd. for $C_{17}H_{16}NO_3$, 282.1125).

Compound **7**: red powder; UV ($CHCl_3$) λ_{max} (log ε) 267 (4.35), 318 (4.17), 334 (4.20), 434 (4.92) nm. IR ν_{max} 3417, 2962, 2918, 2851, 1724, 1600, 1563, 1468, 1445, 1407, 1261, 1092, 1038, 863, 802, 705 cm^{-1}. ^{13}C and ^1H NMR data are shown in Tables S4 and S6. ESI-MS *m/z* 296 $[M+H]^+$ and 294 $[M-H]^-$. HRESIMS *m/z* 296.1276 $[M+H]^+$ (Calcd. for $C_{18}H_{18}NO_3$, 296.1281).

Compound **8**: red powder; UV ($CHCl_3$) λ_{max} (log ε) 268 (3.75), 319 (3.60), 334 (3.84), 434 (4.28) nm. IR ν_{max} 3371, 3207, 2961, 2923, 2853, 1634, 1584, 1554, 1474, 1405, 1374, 1262, 1155, 1096, 1029, 981, 800, 724 cm^{-1}. ^{13}C and ^1H NMR data are shown in Tables S4 and S6. ESI-MS *m/z* 310 $[M+H]^+$ and 308 $[M-H]^-$. HRESIMS *m/z* 310.1425 $[M+H]^+$ (Calcd. for $C_{19}H_{20}NO_3$, 310.1438).

To isolate auxarconjugatin D (**9**), compound **10**, and 12*E*-dechloroisorumbrin (**11**), the spores of strain *AN-rumCDEF* were cultured in 6 L CD-ST agar media containing **5** (2 mmol/L) as substrate and cultured for 7 days at 28 °C. The culture was extracted with EtOAc to give the crude extract (3.8 g), which was partitioned between CH_3OH and PE (1:1, *v/v*). The CH_3OH layer extract (3.4 g) was purified by BUCHI REV Prep with a gradient subjected CH_3OH/H_2O (30:70 to 100:0) to afford six fractions (Frs. 1−6). Fr. 4 (330 mg) was separated by semi-preparative HPLC (CH_3OH/H_2O, 72:28, 0.02% formic acid) to obtain **9** (2.2 mg, t_R = 24.5 min), **10** (1.0 mg, t_R = 27.0 min) and **11** (70.0 mg, t_R = 37.5 min).

Auxarconjugatin D (**9**): red powder; ESI-MS *m/z* 296 $[M+H]^+$. ^{13}C and ^1H NMR data are shown in Tables S4 and S6.

Compound **10**: red powder; UV (MeCN) λ_{max} (log ε) 269 (3.99), 338 (3.84), 454 (4.42) nm. IR ν_{max} 3340, 2962, 2920, 2852, 1712, 1661, 1628, 1538, 1412, 1261, 1095, 1037, 863, 801, 705 cm^{-1}. ^{13}C and ^1H NMR data are shown in Tables S4 and S7. ESI-MS *m/z* 310 $[M+H]^+$ and 308 $[M-H]^-$. HRESIMS *m/z* 310.1433 $[M+H]^+$ (Calcd. for $C_{19}H_{20}NO_3$, 310.1438).

12*E*-dechloroisorumbrin (**11**): red powder; ESI-MS *m/z* 323 $[M+H]^+$. ^{13}C and ^1H NMR data are shown in Tables S4 and S7.

To isolate 12*E*-demethylisorumbrin (**13**) and compound **14**, the spores of *A. nidulans* strain *AN-rumCDEH* were cultured in 8 L CD-ST agar media with **5** (2 mmol/L) as substrate and grown for 6 days at 28 °C. The culture was exhaustively extracted with EtOAc to obtain the crude extract (6.8 g), which was partitioned between CH_3OH and *n*-hexane. The CH_3OH layer extract was purified by BUCHI REV Prep with a gradient subjected CH_3OH/H_2O (30:70 to 100:0) to afford seven fractions (Frs. 1−7). Fr. 4 (320 mg) was separated by semi-preparative HPLC (MeCN/H_2O, 53:47, 0.02% formic acid) to obtain **13** (1.2 mg, t_R = 20.7 min) and **14** (5.83 mg, t_R = 24.8 min).

12*E*-demethylisorumbrin (**13**): red powder; ^{13}C and ^1H NMR data are shown in Tables S4 and S7. ESI-MS *m/z* 330 $[M+H]^+$ and 328 $[M-H]^-$. HRESIMS *m/z* 328.0749 $[M-H]^-$ (Calcd. for $C_{18}H_{15}ClNO_3$, 328.0746).

Compound **14**: red powder; UV (MeCN) λ_{max}: 269, 322, 339, 430 nm. ^{13}C and ^1H NMR data are shown in Tables S4 and S7. ESI-MS *m/z* 344 $[M+H]^+$ and 342 $[M-H]^-$. HRESIMS *m/z* 342.0904 $[M-H]^-$ (Calcd. for $C_{19}H_{17}ClNO_3$, 342.0902).

To isolate auxarconjugatin E (**15**), the spores of *A. nidulans* strain *AN-rumCDEFH* were inoculated into 5 L CD-ST agar media with **5** (2 mmol/L) as precursor and grown for 7 days at 28 °C. The culture was exhaustively extracted with EtOAc to obtain crude extract (4.3 g), which was partitioned between CH_3OH and PE (1:1, *v/v*). The CH_3OH layer extract was purified by BUCHI REV Prep with a gradient subjected CH_3OH/H_2O (30:70 to 100:0) to afford seven fractions (Frs. 1−7). Fr. 4 (380 mg) was separated by semi-preparative HPLC (CH_3OH/H_2O, 72:28, 0.02% formic acid) to yield **15** (0.9 mg, t_R = 27.0 min).

Auxarconjugatin E (**15**): red powder; ^{13}C and ^1H NMR data are shown in Supporting Information Tables S5 and S7. ESI-MS *m/z* 344 $[M+H]^+$ and 342 $[M-H]^-$. HRESIMS *m/z* 344.1042 $[M+H]^+$ (Calcd. For $C_{19}H_{19}O_3NCl$, 344.1048).

To isolate compound **16**, the spores of the *A. nidulans* strain expressing *rumCDE* were inoculated into 10 L CD-ST agar media with **5a** (2 mmol/L) as precursor and grown for 7 days at 28 °C. The culture was exhaustively extracted with EtOAc to obtain crude extract (11 g), which was partitioned between CH_3OH and PE (1:1, *v/v*). The CH_3OH layer extract (10 g) was purified by BUCHI REV Prep with a gradient subjected CH_3OH/H_2O (30:70 to 100:0) to obtain 22 fractions (Frs. 1−22). Frs. 13−19 was combined (232 mg) and separated by semi-preparative HPLC (MeCN/H_2O, 53:47, 0.02% formic acid) to yield **16** (5.9 mg, t_R = 19.2 min).

Compound **16**: red powder; UV (MeCN) λ_{max}: 266, 320, 332, 430 nm. ^{13}C and ^1H NMR data are shown in Tables S5 and S7. ESI-MS *m/z* 328 $[M+H]^+$ and 326 $[M-H]^-$. HRESIMS *m/z* 328.1339 $[M+H]^+$ (Calcd. for $C_{19}H_{19}FNO_3$, 328.1343).

To isolate compounds **17** and **18**, the spores of the *A. nidulans* strain expressing *rumCDEFH* were inoculated into 5 L CD-ST solid media containing **5a** (2 mmol/L), and grown for 6 days at 28 °C. The culture was exhaustively extracted with EtOAc to obtain the crude extract (3.3 g), which was redissolved with *n*-hexane. The residue (3 g) was purified by BUCHI REV Prep with a gradient subjected CH_3OH/H_2O (30:70 to 100:0) to afford eight fractions (Frs. 1−8). Fr. 6 (7 mg) was separated by semi-preparative HPLC (MeCN/H_2O, 60:40, 0.02% formic acid) to yield **17** (1.28 mg, t_R = 23.2 min). Fr. 4 (5 mg) was separated by semi-preparative HPLC (MeCN/H_2O, 65:35, 0.02% formic acid) to yield **18** (1.15 mg, t_R = 16.3 min).

Compound **17**: red powder; UV (MeCN) λ_{max}: 270, 322, 338, 437 nm. ^{13}C and ^1H NMR data are shown in Supporting Information Tables S5 and S8. ESI-MS *m/z* 342 $[M+H]^+$ and 340 $[M-H]^-$. HRESIMS *m/z* 342.1495 $[M+H]^+$ (Calcd. for $C_{20}H_{21}FNO_3$, 342.1500).

Compound **18**: red powder; UV (MeCN) λ_{max}: 261, 312, 329, 435 nm. ^{13}C and ^1H NMR data are shown in Tables S5 and S8. ESI-MS *m/z* 314 $[M+H]^+$ and 312 $[M-H]^-$. HRESIMS: *m/z* 314.1185 $[M+H]^+$ (Calcd. for $C_{18}H_{17}FNO_3$, 314.1187).

To isolate compounds **19**−**21** and 3-floroisorumbrin (**22**), the spores of the *A. nidulans* strain expressing *rumCDEFH* were inoculated into 5 L CD-ST agar media containing **5c** (2 mmol/L), and grown for 6 days at 28 °C. The culture was exhaustively extracted with EtOAc to obtain the crude extract (10.2 g). The crude extract was redissolved with *n*-hexane and the residue (9 g) was purified by BUCHI REV Prep with a gradient subjected CH_3OH/H_2O (30:70 to 100:0) to afford 10 fractions (Frs. 1−10). Fr. 6 (40 mg) was separated by semi-preparative HPLC (MeCN/H_2O, 53:47, 0.02% formic acid) to yield **20** (1.54 mg, t_R = 28.7 min), **21** (11.4 mg, t_R = 24.3 min) and **22** (3.21 mg, t_R = 23.1 min). Fr. 8 (60 mg) was separated by semi-preparative HPLC (MeCN/H_2O, 65:35, 0.02% formic acid) to yield **19** (23.5 mg, t_R = 26.5 min).

Compound **19**: red powder; UV (MeCN) λ_{max}: 261, 325, 339, 430 nm. ^{13}C and ^1H NMR data are shown in Tables S5 and S8. ESI-MS *m/z* 376 $[M+H]^+$ and 374 $[M-H]^-$. HRESIMS *m/z* 376.1108 $[M+H]^+$ (calcd for $C_{20}H_{20}ClFNO_3$, 376.1110).

Compound **20**: red powder; UV (MeCN) λ_{max}: 267, 324, 339, 432 nm. ^{13}C and ^1H NMR data are shown in Tables S5 and S8. ESI-MS *m/z* 362 $[M+H]^+$ and 360 $[M-H]^-$. HRESIMS *m/z* 362.0955 $[M+H]^+$ (Calcd. For $C_{19}H_{18}ClFNO_3$, 362.0954).

Compound **21**: red powder; UV (MeCN) λ_{max}: 262, 315, 330, 426 nm. ^{13}C and ^1H NMR data are shown in Tables S5 and S8. ESI-MS *m/z* 348 $[M+H]^+$ and 346 $[M-H]^-$. HRESIMS *m/z* 348.0795 $[M+H]^+$ (Calcd. for $C_{18}H_{16}ClFNO_3$, 348.0797).

3-Floroisorumbrin (**22**): red powder; ^{13}C and ^1H NMR data are shown in Tables S5 and S8. ESI-MS *m/z* 342 $[M+H]^+$ and 340 $[M-H]^-$. HRESIMS *m/z* 342.1502 $[M+H]^+$ (Calcd. for $C_{20}H_{20}FNO_3$, 342.1500).

To isolate 3-bromoisorumbrin (**23**) and compound (**24**), the spores of the *A. nidulans* strain expressing *rumCDEFH* were inoculated into 5 L CD-ST agar media containing **5e** (2 mmol/L), and grown for 6 days at 28 °C. The culture was exhaustively extracted with EtOAc to obtain the crude extract (5.2 g), which was redissolved with *n*-hexane. The residue (5 g) was purified by BUCHI REV Prep with a gradient subjected CH_3OH/H_2O (30:70 to 100:0) to afford six fractions (Frs. 1−6). Fr. 6 (32 mg) was separated by semi-preparative HPLC (MeCN/H_2O, 70:30, 0.02% formic acid) to yield **23** (1.7 mg, t_R = 17.5 min). Fr. 4 (24 mg) was separated by semi-preparative HPLC (MeCN/H_2O, 75:25, 0.02% formic acid) to yield **24** (1.0 mg, t_R = 25.5 min).

3-Bromoisorumbrin (**23**): red powder; ^{13}C and ^1H NMR data are shown in Tables S5 and S8. ESI-MS *m/z* 403 $[M+H]^+$ and 401 $[M-H]^-$.

Compound **24**: red powder; (MeCN) λ_{max}: 247, 301, 414 nm. ^{13}C and ^1H NMR data are shown in Supporting Information Tables S5 and S9. ESI-MS *m/z* 349 $[M+H]^+$ and 347 $[M-H]^-$. HRESIMS *m/z* 348.0234 $[M+H]^+$ (Calcd. for $C_{16}H_{15}BrNO_3$, 348.0230).

To isolation of compound **25**, the spores of the *A. nidulans* strain expressing *malACDEF* were inoculated into 9.5 L CD-ST

agar media containing **5** (2 mmol/L), and grown for 7 days at 28 °C. The culture was exhaustively extracted with EtOAc to give the crude extract (3.5 g), which was redissolved with petroleum ether (PE). The residue (3 g) was purified by BUCHI REV Prep with a gradient subjected CH_3OH/H_2O (30:70 to 100:0) to afford 15 fractions (Frs. 1−15). Fr. 12 (46 mg) was separated by semi-preparative HPLC ($MeCN/H_2O$, 38:62, 0.02% formic acid) to yield **25** (6.0 mg, t_R = 18.1 min).

Compound **25**: dark colored amorphous powder; UV (MeCN) λ_{max}: 230, 295, 410 nm. ^{13}C and ^{1}H NMR data are shown in Supporting Information Table S6. HRESIMS *m/z* 292.0736 $[M+H]^+$ (Calcd. for $C_{15}H_{15}ClNO_3$, 292.0735).

4.10. Anti-HIV assay

4.10.1. Cell culture

HEK293T and SupT1 cells were maintained in DMEM and RPMI1640 supplemented with 10% fetal bovine serum (FBS), respectively.

4.10.2. Plasmids and reagents

The HIV pNL4-3Luc.R-E- vector encodes for a full-length HIV-1 proviral DNA, in which luciferase gene is inserted as a reporter and env is defective. A plasmid pHIT/G expressing the vesicular stomatitis virus glycoprotein (VSV-G) was provided by Johnny He[24].

4.10.3. Viral preparation and assay for the inhibitory activity measurement of compounds

In short, 2×10^5 HEK293T cells were co-transfected with 0.4 μg of pHIT/G and 0.6 μg of pNL4-3Luc.R-E-. The pseudotyped HIV-1 viruses were harvested by filtration followed by the quantification of viral capsid protein by p24 antigen capture ELISA. The resulting viruses were used to infect a total of 5×10^5 SupT1 cells at an MOI of 1, in the presence of compounds at serial dilutions. After further incubation at 37 °C, 5% CO_2 for 48 h, a firefly luciferase assay system (Promega, Madison, WI, USA) was performed to determine the inhibition rate.

4.10.4. Semi-quantitative real-time PCR

VSV-G pseudotyped NL4-3Luc.R-E- viruses were used to infect a total of 5×10^6 SupT1 cells treated with 4 nmol/L efavirenz (EFV), 25 nmol/L raltegravir (RAL) or test compounds (10 times IC_{50}). Cells were harvested at 24 h and subjected to total DNA extraction by DNeasy Blood&Tissue Kit (Qiagen). An aliquot of each sample was analyzed by quantitative PCR. The primers used in the PCR were listed in Table S1. Copy numbers of total viral DNA, integrated DNA, and 2-LTR were normalized by that of the GAPDH gene.

Acknowledgments

This work was supported financially by the National Key Research and Development Program of China (2018YFA0901900), and the CAMS Innovation Fund for Medical Sciences (CIFMS, No. 2021-I2M-1-029, China).

Author contributions

Beifen Zhong conducted experiments, bioinformatics analysis and wrote the manuscript; Jun Wang constituted the skeleton and post-PKS modification pathway of rumbrin; Changhui Shang performed the isolations and structural elucidation of compounds from heterologous expression and wrote the manuscript; Jiajia Wen and Yujia Wang performed anti-HIV assays; Jian Bai involved in NMR data analysis; Shan Cen designed the anti-HIV assays, discussed the project and edited the manuscript; Youcai Hu designed and guided the entire project and edited the manuscript.

Conflicts of interest

The authors declare no conflicts of interest.

Appendix A. Supporting information

Supporting data to this article can be found online at https://doi.org/10.1016/j.apsb.2022.02.005.

References

1. Shen B. A new golden age of natural products drug discovery. *Cell* 2015;**163**:1297−300.
2. Newman DJ, Cragg GM. Natural products as sources of new drugs over the nearly four decades from 01/1981 to 09/2019. *J Nat Prod* 2020;**83**:770−803.
3. Bai J, Mu R, Dou M, Yan D, Liu B, Wei Q, et al. Epigenetic modification in histone deacetylase deletion strain of *Calcarisporium arbuscula* leads to diverse diterpenoids. *Acta Pharm Sin B* 2018;**8**:687−9.
4. Wei Q, Bai J, Yan D, Bao X, Li W, Liu B, et al. Genome mining combined metabolic shunting and OSMAC strategy of an endophytic fungus leads to the production of diverse natural products. *Acta Pharm Sin B* 2021;**11**:572−87.
5. Alanjary M, Kronmiller B, Adamek M, Blin K, Weber T, Huson D, et al. The antibiotic resistant target seeker (ARTS), an exploration engine for antibiotic cluster prioritization and novel drug target discovery. *Nucleic Acids Res* 2017;**45**:W42−8.
6. Lautru S, Deeth RJ, Bailey LM, Challis GL. Discovery of a new peptide natural product by *Streptomyces coelicolor* genome mining. *Nat Chem Biol* 2005;**1**:265−9.
7. Yan Y, Liu Q, Zang X, Yuan S, Bat-Erdene U, Nguyen C, et al. Resistance-gene-directed discovery of a natural-product herbicide with a new mode of action. *Nature* 2018;**559**:415−8.
8. Panter F, Krug D, Baumann S, Müller R. Self-resistance guided genome mining uncovers new topoisomerase inhibitors from myxobacteria. *Chem Sci* 2018;**9**:4898−908.
9. Yan Y, Liu N, Tang Y. Recent developments in self-resistance gene directed natural product discovery. *Nat Prod Rep* 2020;**37**:879−92.
10. Wang J, Zhang R, Chen X, Sun X, Yan Y, Shen X, et al. Biosynthesis of aromatic polyketides in microorganisms using type II polyketide synthases. *Microb Cell Factories* 2020;**19**:110.
11. Waldman AJ, Balskus EP. Lomaiviticin biosynthesis employs a new strategy for starter unit generation. *Org Lett* 2014;**16**:640−3.
12. Abe I, Utsumi Y, Oguro S, Morita H, Sano Y, Noguchi H. A plant type III polyketide synthase that produces pentaketide chromone. *J Am Chem Soc* 2005;**127**:1362−3.
13. Crawford JM, Vagstad AL, Ehrlich KC, Townsend CA. Starter unit specificity directs genome mining of polyketide synthase pathways in fungi. *Bioorg Chem* 2008;**36**:16−22.
14. Zhang M, Hou XF, Qi LH, Yin Y, Li Q, Pan HX, et al. Biosynthesis of trioxacarcin revealing a different starter unit and complex tailoring steps for type II polyketide synthase. *Chem Sci* 2015;**6**:3440−7.
15. Kalaitzis JA, Cheng Q, Thomas PM, Kelleher NL, Moore BS. *In vitro* biosynthesis of unnatural enterocin and wailupemycin polyketides. *J Nat Prod* 2009;**72**:469−72.
16. Hong H, Fill T, Leadlay PF. A common origin for guanidinobutanoate starter units in antifungal natural products. *Angew Chem Int Ed Engl* 2013;**52**:13096−9.

17. Hu DX, Withall DM, Challis GL, Thomson RJ. Structure, chemical synthesis, and biosynthesis of prodiginine natural products. *Chem Rev* 2016;**116**:7818−53.
18. Dorrestein PC, Yeh E, Garneau-Tsodikova S, Kelleher NL, Walsh CT. Dichlorination of a pyrrolyl-*S*-carrier protein by $FADH_2$-dependent halogenase PltA during pyoluteorin biosynthesis. *Proc Natl Acad Sci U S A* 2005;**102**:13843−8.
19. Yamagishi Y, Matsuoka M, Odagawa A, Kato S, Shindo K, Mochizuki J. Rumbrin, a new cytoprotective substance produced by *Auxarthron umbrinum*. I. Taxonomy, production, isolation and biological activities. *J Antibiot (Tokyo)* 1993;**46**:884−7.
20. Clark BR, Capon RJ, Lacey E, Tennant S, Gill JH. Polyenylpyrroles and polyenylfurans from an Australian isolate of the soil ascomycete *Gymnoascus reessii*. *Org Lett* 2006;**8**:701−4.
21. Fang Z, Liao PC, Yang YL, Yang FL, Chen YL, Lam Y, et al. Synthesis and biological evaluation of polyenylpyrrole derivatives as anticancer agents acting through caspases-dependent apoptosis. *J Med Chem* 2010;**53**:7967−78.
22. Clark BR, Murphy CD. Biosynthesis of pyrrolylpolyenes in *Auxarthron umbrinum*. *Org Biomol Chem* 2009;**7**:111−6.
23. Clark BR, O'Connor S, Fox D, Leroy J, Murphy CD. Production of anticancer polyenes through precursor-directed biosynthesis. *Org Biomol Chem* 2011;**9**:6306−11.
24. Levin A, Armon-Omer A, Rosenbluh J, Melamed-Book N, Graessmann A, Waigmann E, et al. Inhibition of HIV-1 integrase nuclear import and replication by a peptide bearing integrase putative nuclear localization signal. *Retrovirology* 2009;**6**:112.
25. Yamagishi Y, Shindo K, Kawai H. Rumbrin, a new cytoprotective substance produced by *Auxarthron umbrinum*. II. Physico-chemical properties and structure determination. *J Antibiot (Tokyo)* 1993;**46**:888−91.
26. Lin TS, Chiang YM, Wang CC. Biosynthetic pathway of the reduced polyketide product citreoviridin in *Aspergillus terreus* var. aureus revealed by heterologous expression in *Aspergillus nidulans*. *Org Lett* 2016;**18**:1366−9.
27. Skellam E. Biosynthesis of fungal polyketides by collaborating and trans-acting enzymes. *Nat Prod Rep* 2022;**39**:754−83.
28. Zhang Y, Bai J, Zhang L, Zhang C, Liu B, Hu Y. Self-resistance in the biosynthesis of fungal macrolides involving cycles of extracellular oxidative activation and intracellular reductive inactivation. *Angew Chem Int Ed Engl* 2021;**60**:6639−45.
29. Moore BS, Hertweck C. Biosynthesis and attachment of novel bacterial polyketide synthase starter units. *Nat Prod Rep* 2002;**19**:70−99.
30. Garneau S, Dorrestein PC, Kelleher NL, Walsh CT. Characterization of the formation of the pyrrole moiety during clorobiocin and coumermycin A1 biosynthesis. *Biochemistry* 2005;**44**:2770−80.
31. Garneau-Tsodikova S, Dorrestein PC, Kelleher NL, Walsh CT. Protein assembly line components in prodigiosin biosynthesis: characterization of PigA,G,H,I,J. *J Am Chem Soc* 2006;**128**:12600−1.
32. Thomas MG, Burkart MD, Walsh CT. Conversion of L-proline to pyrrolyl-2-carboxyl-*S*-PCP during undecylprodigiosin and pyoluteorin biosynthesis. *Chem Biol* 2002;**9**:171−84.
33. Fraley AE, Garcia-Borràs M, Tripathi A, Khare D, Mercado-Marin EV, Tran H, et al. Function and structure of MalA/MalA', iterative halogenases for late-stage C-H functionalization of indole alkaloids. *J Am Chem Soc* 2017;**139**:12060−8.
34. Murphy CD, Clark BR, Amadio J. Metabolism of fluoroorganic compounds in microorganisms: impacts for the environment and the production of fine chemicals. *Appl Microbiol Biotechnol* 2009;**84**:617−29.
35. Deb Roy A, Grüschow S, Cairns N, Goss RJ. Gene expression enabling synthetic diversification of natural products: chemogenetic generation of pacidamycin analogs. *J Am Chem Soc* 2010;**132**:12243−5.
36. Kale AJ, McGlinchey RP, Lechner A, Moore BS. Bacterial self-resistance to the natural proteasome inhibitor salinosporamide A. *ACS Chem Biol* 2011;**6**:1257−64.
37. Yeh HH, Ahuja M, Chiang YM, Oakley CE, Moore S, Yoon O, et al. Resistance gene-guided genome mining: serial promoter exchanges in *Aspergillus nidulans* reveal the biosynthetic pathway for fellutamide B, a proteasome inhibitor. *ACS Chem Biol* 2016;**11**:2275−84.
38. Thaker MN, Wang W, Spanogiannopoulos P, Waglechner N, King AM, Medina R, et al. Identifying producers of antibacterial compounds by screening for antibiotic resistance. *Nat Biotechnol* 2013;**31**:922−7.
39. Tang X, Li J, Millán-Aguiñaga N, Zhang JJ, O'Neill EC, Ugalde JA, et al. Identification of thiotetronic acid antibiotic biosynthetic pathways by target-directed genome mining. *ACS Chem Biol* 2015;**10**:2841−9.
40. Yarlagadda V, Medina R, Johnson TA, Koteva KP, Cox G, Thaker MN, et al. Resistance-guided discovery of elfamycin antibiotic producers with antigonococcal activity. *ACS Infect Dis* 2020;**6**:3163−7.
41. O'Neill EC, Schorn M, Larson CB, Millán-Aguiñaga N. Targeted antibiotic discovery through biosynthesis-associated resistance determinants: target directed genome mining. *Crit Rev Microbiol* 2019;**45**:255−77.
42. Almabruk KH, Dinh LK, Philmus B. Self-resistance of natural product producers: past, present, and future focusing on self-resistant protein variants. *ACS Chem Biol* 2018;**13**:1426−37.
43. Li J, Derewenda U, Dauter Z, Smith S, Derewenda ZS. Crystal structure of the *Escherichia coli* thioesterase II, a homolog of the human Nef binding enzyme. *Nat Struct Biol* 2000;**7**:555−9.
44. Liu LX, Margottin F, Le Gall S, Schwartz O, Selig L, Benarous R, et al. Binding of HIV-1 Nef to a novel thioesterase enzyme correlates with Nef-mediated CD4 down-regulation. *J Biol Chem* 1997;**272**:13779−85.
45. Dillon SC, Bateman A. The hotdog fold: wrapping up a superfamily of thioesterases and dehydratases. *BMC Bioinf* 2004;**5**:109.
46. Ding J, Zhao J, Yang Z, Ma L, Mi Z, Wu Y, et al. Microbial natural product alternariol 5-*O*-methyl ether inhibits HIV-1 integration by blocking nuclear import of the pre-integration complex. *Viruses* 2017;**9**:105.
47. Palmeira JDF, Argañaraz GA, de Oliveira G, Argañaraz ER. Physiological relevance of ACOT8-Nef interaction in HIV infection. *Rev Med Virol* 2019;**29**:e2057.
48. Hunt MC, Solaas K, Kase BF, Alexson SE. Characterization of an acyl-coA thioesterase that functions as a major regulator of peroxisomal lipid metabolism. *J Biol Chem* 2002;**277**:1128−38.
49. Staudt RP, Alvarado JJ, Emert-Sedlak LA, Shi H, Shu ST, Wales TE, et al. Structure, function, and inhibitor targeting of HIV-1 Nef-effector kinase complexes. *J Biol Chem* 2020;**295**:15158−71.